Thermoelastic Stresses in Balanced and Unbalanced Seals

By T. D. RINEY and J. W. ELEK

(Manuscript received April 28, 1961)

This paper presents the results of a two-part analytical study of the stresses produced when ceramic cylinders are butt sealed to metal washer plates. Such stacked structures are of increasing importance in the fabrication of encapsulations for electron tubes and semiconductor devices.

Practical experience, rather than analysis, has shown the advantage of a balanced seal and it is now in common usage in the electronic industry. In some applications other requirements may prevent direct back-to-back balancing and the question arises as to how much the diameters of the opposing seals may differ and still give the desired balanced effect. In Sections 3.1, 4.1, and 5.1 this question is considered and the concept of a balanced seal is placed on a firmer basis. The results indicate that a small difference in the radii is to be preferred.

The effect of the length of an intermediate cylinder on the stresses in a three-cylinder stacked structure is considered in Sections 3.2, 4.2, and 5.2.

I. INTRODUCTION

In the electronic industry ceramic-to-metal seals are of increasing importance in the fabrication of encapsulations for electron tubes and semiconductor devices. The most common method for sealing ceramics to metals is to first "metallize" the ceramic by sintering onto it a thin coating of metallic powder; common brazing materials such as gold-copper alloys, silver-copper alloys, etc. are then used to fasten the metallized ceramic to the metal.

Temperatures in excess of 500°C are required for the brazing operation. As the assembly cools from the set-point of the brazing material to room temperature, thermoelastic stresses are induced in the bonded components by the differences in their thermal contraction rates. These stresses must be controlled if physical distortion and the resultant possibility of bond failure or fracture of the metal or ceramic are to be avoided.

Their magnitude depends on the choice of metal, ceramic, and brazing material as well as the applied heat treatment. If it is assumed that these parameters are held fixed, the magnitude of the thermoelastic stresses will still vary widely as a function of the structure geometry.

This paper presents the results of a two-part analytical study of the stresses produced when ceramic cylinders are butt sealed to metal washer plates. The problems considered are represented by the electron tube envelope assembly depicted in Fig. 1. At position A the top ceramic cylinder is used to balance the effect of the ceramic-metal seal on the other side; it serves no other purpose. Practical experience, rather than analysis, has shown the advantages of a balanced seal and it is now in common usage in the industry. In some applications other requirements may prevent direct back-to-back balancing (as at position C) and the question arises as to how much the diameters of the opposing seals may differ and still give the balanced effect. In the first part of the paper this question is considered and the concept of a balanced seal is placed on a firmer basis.

At position B the question arises as to the effect that the length of the middle cylinder has on the stresses produced. This problem is treated

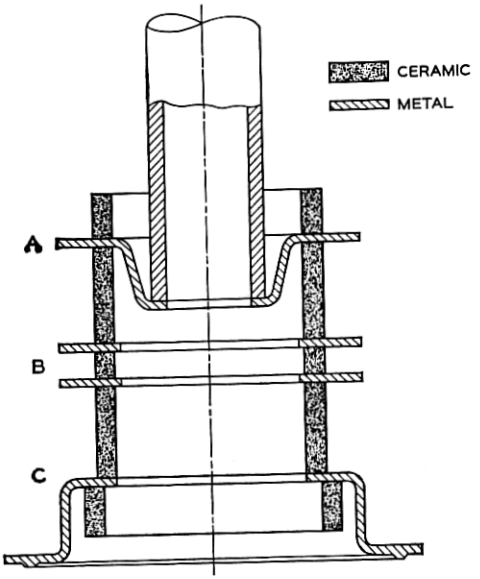

Fig. 1 — A cross-sectional view of a representative ceramic-metal electron tube envelope.

in Sections 3.2, 4.2, and 5.2. A similar study of the effects of the intermediate lengths in a graded cylindrical butt seal has been reported.[1–4] Another related problem is a long pipe reinforced by rings and submitted to the action of uniform internal pressure.[5] The thread that holds together these problems and the problem considered in Sections 3.1, 4.1, and 5.1 is that the stresses are produced by bonding together parts that would ordinarily be discontinuous at the joints under the given conditions. The continuity is produced by distributed forces and moments acting on each component along the joint.

II. ASSUMPTIONS AND NOTATIONS

Discontinuity stresses are highly localized; they are attenuated rapidly as the distance from the joint increases. Certain of the dimensions of the structure may therefore be idealized as infinite in extent without significantly affecting the stress distribution. The calculations are thereby greatly simplified. The idealized configurations for the two parts of the study are shown in Fig. 2.

The metal and ceramic bodies are imagined to be sealed together at a temperature T_0, the temperature then lowered to room value, T. It is assumed that no external restraining forces act on the structure during the sealing and cooling. The distributed forces, Q_i, and bending

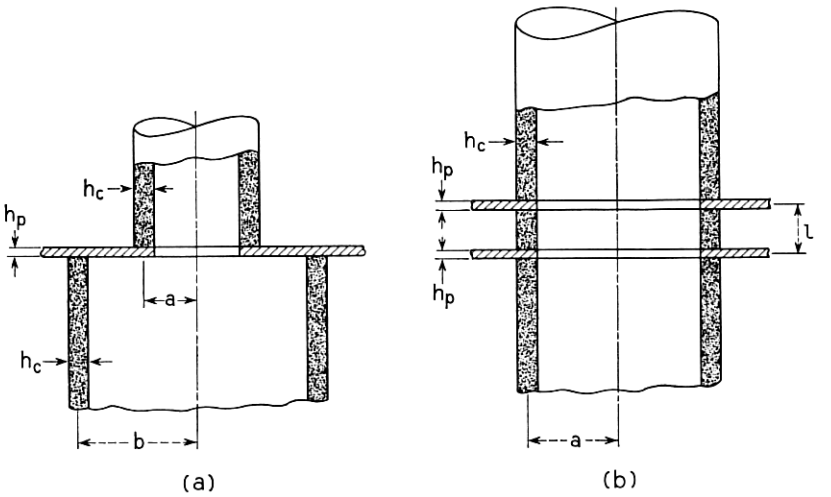

Fig. 2 — Cross-sectional view of the structures idealized to study: (a) the effects of a balanced seal; (b) the effect of varying l.

moments, M_i, required to maintain continuity at the joints of the ceramic-metal seals are depicted in the exploded diagrams of Fig. 3. The positive direction for the deflections and displacements are also shown.

To evaluate the edge loadings it is expedient to refer to the literature for the appropriate expressions for the deflections, displacements and slopes. This will be done freely. The formulas are based on the membrane theory of cylinders and plates, i.e., diameter to thickness ratio $\geqq 5$. It is also assumed that the deflections are small enough that the radial loads on the plates have negligible bending effects. In using these expressions the following notations will be employed:

$$D_c = \frac{E_c h_c^3}{12(1-\nu_c^2)} \qquad D_p = \frac{E_p h_p^3}{12(1-\nu_p^2)} \qquad R = \frac{E_c}{E_p} \tag{1}$$

$$\beta_1^4 = \frac{E_c h_c}{4a^2 D_c} \qquad \beta_2^4 = \frac{E_c h_c}{4b^2 D_c} \qquad \Delta = E_c(\alpha_c - \alpha_p)(T - T_0)$$

where E is the elastic modulus; ν Poisson's ratio, and the subscripts c and p indicate cylinder and plate, respectively.

Once the edge loadings have been calculated the results will then be used to evaluate the stresses that they produce in the ceramic cylinders. The notations used for the stresses are illustrated in Fig. 4. In calculating

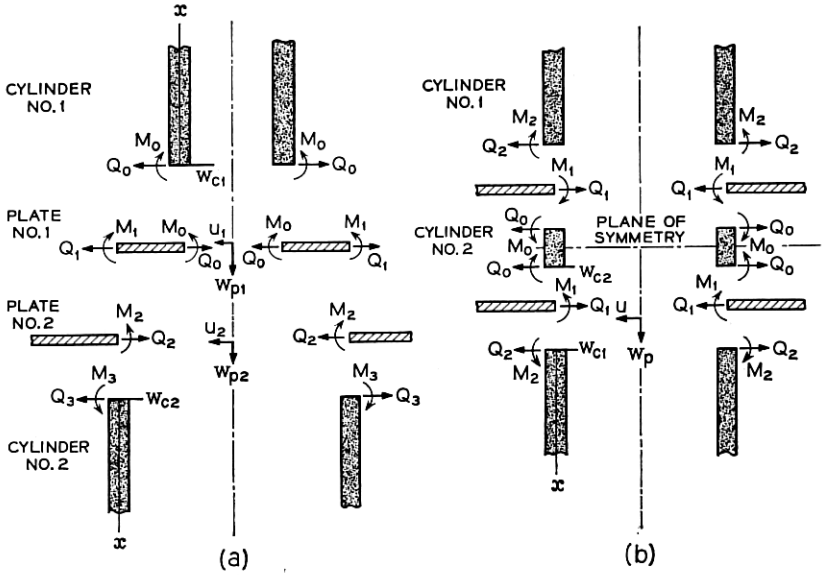

Fig. 3 — Exploded views showing the notations used for the moments and deflections.

the stress values the literature on cylindrical shell theory uses the following standard notation:

$$\begin{aligned} \varphi &= e^{-\beta x}(\cos \beta x + \sin \beta x) & \theta &= e^{-\beta x} \cos \beta x \\ \psi &= e^{-\beta x}(\cos \beta x - \sin \beta x) & \zeta &= e^{-\beta x} \sin \beta x \end{aligned} \tag{2}$$

and

$$\chi_1(\beta l) = \frac{\cosh \beta l + \cos \beta l}{\sinh \beta l + \sin \beta l} \qquad \chi_2(\beta l) = \frac{\sinh \beta l - \sin \beta l}{\sinh \beta l + \sin \beta l}$$
$$\chi_3(\beta l) = \frac{\cosh \beta l - \cos \beta l}{\sinh \beta l + \sin \beta l}. \tag{3}$$

III. FORMULATION OF PROBLEMS

The problem considered in the first part of this and the following two sections is essentially the effect of radial unbalance in butt seals. The second is concerned with an axial unbalance resulting from the finite length of the intermediate cylinder. At this point it seems desirable to treat the problems separately.

3.1 *Radial Unbalance*

Static equilibrium at the joint $r = b$, Fig. 3(a), requires that

$$Q_2 = Q_1 + Q_3 \qquad M_2 = M_1 - M_3 \tag{4}$$

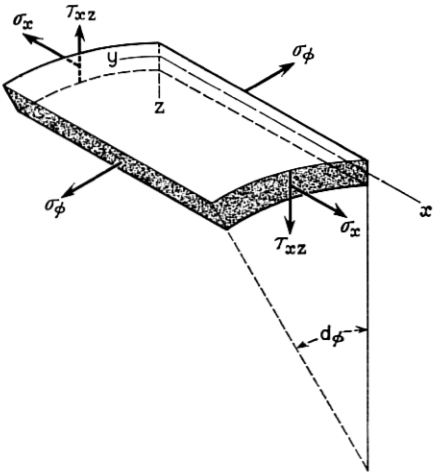

Fig. 4 — Cylindrical element showing stress directions.

and the quantities to be determined are reduced to six: Q_0, Q_1, Q_3, M_0, M_1, M_3. These will be evaluated by using the boundary conditions that at the juncture of the cylinders and plate the radial displacements are the same and the plate remains perpendicular to the cylinders. The following six conditions are obtained:

(a) The radial displacement of cylinder #1 and plate #1 are equal along the junction at $r = a$.
(b) The radial displacement of the two plates is the same at $r = b$.
(c) The radial displacement of cylinder #2 and plate #2 are equal along the junction at $r = b$.
(d) Cylinder #1 and plate #1 remain at right angles at their juncture.
(e) The slope of the two plates is the same at $r = b$.
(f) Cylinder #2 and plate #2 remain at right angles at their juncture.

The radial displacement of each part consists of a term due to the temperature change and a term due to the constraint forces resulting from the temperature change. Using the standard notations for displacements as depicted in Fig. 3(a), the first three conditions may be expressed symbolically as follows:

$$\begin{aligned} -(w_{c1})_{x=0} + a\alpha_c(T - T_0) &= (u_1)_{r=a} + a\alpha_p(T - T_0) \\ (u_1)_{r=b} + b\alpha_p(T - T_0) &= (u_2)_{r=b} + b\alpha_p(T - T_0) \\ -(w_{c2})_{x=0} + b\alpha_c(T - T_0) &= (u_2)_{r=b} + b\alpha_p(T - T_0). \end{aligned} \tag{5}$$

From the sketches in Fig. 5(a) it may be seen that the last three conditions yield the following relationships:

$$\begin{aligned} \gamma_a = -\left(\frac{dw_{c1}}{dx}\right)_{x=0} = \left(\frac{dw_{p1}}{dr}\right)_{r=a} \qquad -\gamma_b = \left(\frac{dw_{p1}}{dr}\right)_{r=b} = \left(\frac{dw_{p2}}{dr}\right)_{r=b} \\ -\gamma_b = \left(\frac{dw_{c2}}{dx}\right)_{x=0} = \left(\frac{dw_{p2}}{dr}\right)_{r=b}. \end{aligned} \tag{6}$$

It is now required to express the deflections and their derivatives appearing in (5) and (6) in terms of the unknown quantities Q_0, Q_1, $\cdots$, M_3. From Timoshenko (see Ref. 5, p. 393) it is found that

$$\begin{aligned} (w_{c1})_{x=0} = -\frac{1}{2\beta_1^3 D_c}[\beta_1 M_0 + Q_0] \quad (w_{c2})_{x=0} = -\frac{1}{2\beta_2^3 D_c}[\beta_2 M_3 + Q_3] \\ \left(\frac{dw_{c1}}{dx}\right)_{x=0} = \frac{1}{2\beta_1^2 D_c}[2\beta_1 M_0 + Q_0] \quad \left(\frac{dw_{c2}}{dx}\right)_{x=0} = \frac{1}{2\beta_2^2 D_c}[2\beta_2 M_3 + Q_3]. \end{aligned} \tag{7}$$

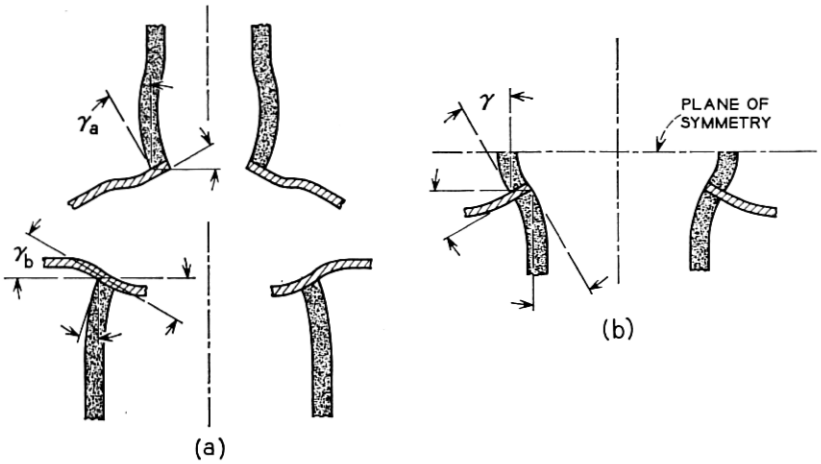

Fig. 5 — Exaggerated picture of deflections produced by discontinuity forces and moments acting at joints.

The forces Q_0 and Q_1, acting on plate #1 produce radial displacement and normal loading given by[6]

$$u_1 = Ar + \frac{B}{r} Q_{p1} = E_p h_p \left[\frac{Ar}{1 - \nu_p} - \frac{B}{1 + \nu_p} \frac{1}{r^2} \right].$$

Here the constants A and B may be determined from the conditions that Q_{p1} attains the value Q_0 and Q_1 at $r = a$ and $r = b$ respectively. If this is done and the values are substituted into the above expression for u_{p1}, one finds

$$(u_1)_{r=a} = \frac{a}{E_p h_p (1 - a^2/b^2)} \{2Q_1 - Q_0[(1 - \nu_p)a^2/b^2 + (1 + \nu_p)]\}$$
$$(u_1)_{r=b} = \frac{b}{E_p h_p (1 - a^2/b^2)} \{Q_1[(1 - \nu_p) + (1 + \nu_p)a^2/b^2] - 2Q_0 a^2/b^2\} \quad (8)$$

If $a \to b$, $b \to \infty$, $Q_0 \to Q_2$, $Q_1 \to 0$, then the first of these gives

$$(u_2)_{r=b} = -\frac{b(1 + \nu_p)}{E_p h_p} Q_2 = -\frac{b(1 + \nu_p)}{E_p h_p} (Q_1 + Q_3). \quad (9)$$

The bending moments along the edges of plate #1 produce slopes (see Ref. 5, p. 63)

$$\left(\frac{dw_{p1}}{dr}\right)_{r=a} = \frac{a}{D_p(1 - a^2/b^2)} \cdot\left\{M_0\left[\frac{a^2/b^2}{1 + \nu_p} + \frac{1}{1 - \nu_p}\right] - M_1\left[\frac{1}{1 + \nu_p} + \frac{1}{1 - \nu_p}\right]\right\}$$

$$\left(\frac{dw_{p1}}{dr}\right)_{r=b} = \frac{b}{D_p(1 - a^2/b^2)} \cdot\left\{M_0\left[\frac{a^2/b^2}{1 + \nu_p} + \frac{a^2/b^2}{1 - \nu_p}\right] - M_1\left[\frac{1}{1 + \nu_p} + \frac{a^2/b^2}{1 - \nu_p}\right]\right\}. \tag{10}$$

If we let $a \to b$, $b \to \infty$, $M_0 \to M_2$, $M_1 \to 0$, then the first of these yields

$$\left(\frac{dw_{p2}}{dr}\right)_{r=b} = \frac{bM_2}{D_p(1 - \nu_p)} = \frac{b}{D_p(1 - \nu_p)}(M_1 - M_3). \tag{11}$$

The required six equations relating $Q_0, \cdots, M_3$ may now be obtained by substituting expressions (7) through (11) into conditions (5) and (6). The resulting equations are simplified and only negligible error introduced if one sets

$$\nu_p = \nu_c = \tfrac{1}{3}.$$

Then

$$D_c = \frac{3E_c h_c^3}{32}, \qquad D_p = \frac{3E_p h_p^3}{32}, \qquad \beta_1^4 = \frac{8}{3a^2 h_c^2}, \qquad \beta_2^4 = \frac{8}{3b^2 h_c^2}$$

and the six equations reduce to

$$\left[\frac{\sqrt{8/3}}{\beta_1 h_c^2} + \frac{R}{3h_p}\frac{2 + a^2/b^2}{1 - a^2/b^2}\right]\frac{Q_0}{\Delta} - \frac{R}{h_p(1 - a^2/b^2)}\frac{Q_1}{\Delta} + \frac{\sqrt{8/3}}{h_c^2}\frac{M_0}{\Delta} = -\tfrac{1}{2}$$

$$-\frac{a^2}{b^2}\frac{Q_0}{\Delta} + \frac{Q_1}{\Delta} + \frac{2}{3}(1 - a^2/b^2)\frac{Q_3}{\Delta} = 0$$

$$\frac{2}{3}\frac{R}{h_p}\frac{Q_1}{\Delta} + \left[\frac{2}{3}\frac{R}{h_p} + \frac{\sqrt{8/3}}{\beta_2 h_c^2}\right]\frac{Q_3}{\Delta} + \frac{\sqrt{8/3}}{h_c^2}\frac{M_3}{\Delta} = -\tfrac{1}{2}$$

$$\frac{2}{a\beta_1^2}\frac{Q_0}{\Delta} + \left[\frac{4}{a\beta_1} + \frac{3Rh_c^3}{h_p^3}\frac{2 + a^2/b^2}{1 - a^2/b^2}\right]\frac{M_0}{\Delta} - \frac{9Rh_c^3}{h_p^3(1 - a^2/b^2)}\frac{M_1}{\Delta} = 0 \tag{12}$$

$$\frac{a^2}{b^2}\frac{M_0}{\Delta} - \frac{M_1}{\Delta} + \frac{2}{3}(1 - a^2/b^2)\frac{M_3}{\Delta} = 0$$

$$\frac{1}{b\beta_2^2}\frac{Q_3}{\Delta} - \frac{3Rh_c^3}{h_p^3}\frac{M_1}{\Delta} + \left[\frac{2}{b\beta_2} + \frac{3Rh_c^3}{h_p^3}\right]\frac{M_3}{\Delta} = 0.$$

3.2 *Axial Unbalance*

Static equilibrium at the joint $r = a$, Fig. 3(b), requires that

$$Q_1 = Q_0 + Q_2 \qquad M_1 = M_0 - M_2 \tag{13}$$

and only the quantities Q_0, Q_2, M_0, M_2 remain to be determined. The four conditions to be satisfied are:

(*a*) The radial displacement of cylinder #1 and the plate are equal along the junction at $r = a$.

(*b*) The radial displacement of cylinder #2 and the plate are equal at $r = a$.

(*c*) Cylinder #1 and the plate remain at right angles along the junction.

(*d*) Cylinder #2 and the plate remain at right angles along the junction.

If we use the notations as defined in Fig. 3(b) the symbolic form of conditions (a) and (b) become

$$\begin{aligned} -(w_{c1})_{x=0} + a\alpha_c(T - T_0) &= (u_p)_{r=a} + a\alpha_p(T - T_0) \\ -(w_{c2})_{x=0} + a\alpha(T - T_0) &= (u_p)_{r=a} + a\alpha_p(T - T_0). \end{aligned} \tag{14}$$

From the sketch shown in Fig. 5(b) we see that the conditions (*c*) and (*d*) yield the relations

$$\gamma = -\left(\frac{dw_{c1}}{dx}\right)_{x=0} = \left(\frac{dw_p}{dr}\right)_{r=a} \qquad \gamma = \left(\frac{dw_{c2}}{dx}\right)_{x=0} = \left(\frac{dw_p}{dr}\right)_{r=a}. \tag{15}$$

The deflections and their derivatives may be written in terms of the unknown quantities Q_0, Q_2, M_0, M_2 as follows (see Ref. 5, p. 403):

$$\begin{aligned} (w_{c1})_{x=0} &= -\frac{2\beta a^2}{E_c h_c}[Q_0\chi_1(\beta l) + \beta M_0\chi_2(\beta l)] \\ \left(\frac{dw_{c1}}{dx}\right)_{x=0} &= \frac{2\beta^2 a^2}{E_c h_c}[Q_0\chi_2(\beta l) + 2\beta M_0\chi_3(\beta l)], \end{aligned} \tag{16}$$

where the notations in (3) are used.

From equations (9) and (11) it is found that in the infinite plate the following relations hold

$$\begin{aligned} (u)_{r=a} &= -\frac{a(1 + \nu_p)}{E_p h_p} \qquad Q_1 = -\frac{a(1 + \nu_p)}{E_p h_p}(Q_0 + Q_2) \\ \left(\frac{dw_p}{dr}\right)_{r=a} &= \frac{a}{D_p(1 - \nu_p)} \qquad M_1 = \frac{a}{D_p(1 - \nu_p)}(M_0 - M_2). \end{aligned} \tag{17}$$

Finally, the cylinder distortions are given by (see Ref. 5, p. 393)

$$\begin{aligned}(w_{c2})_{x=0} &= -\frac{1}{2\beta^3 D_c}[\beta M_2 + Q_2] \\ \left(\frac{dw_{c2}}{dx}\right)_{x=0} &= \frac{1}{2\beta^2 D_c}[2\beta M_2 + Q_2].\end{aligned} \tag{18}$$

The required four equations to determine the unknowns Q_0, Q_2, M_0, M_2 may now be found by substituting expressions (16), (17) and (18) into conditions (14) and (15). If we again set $\nu_p = \nu_c = \frac{1}{3}$, then

$$\beta^4 = \frac{8}{3a^2 h_c^2}$$

and the four equations reduce to

$$\begin{aligned}\left[\frac{a\beta}{h_c}\chi_1(\beta l) + \frac{2R}{3h_p}\right]\frac{Q_0}{\Delta} + \frac{2R}{3h_p}\frac{Q_2}{\Delta} + \frac{\sqrt{8/3}}{h_c^2}\chi_2(\beta l)\frac{M_0}{\Delta} &= -\tfrac{1}{2} \\ \frac{2R}{3h_p}\frac{Q_0}{\Delta} + \left[\frac{2R}{3h_p} + \frac{\sqrt{8/3}}{\beta h_c^2}\right]\frac{Q_2}{\Delta} + \frac{\sqrt{8/3}}{h_c^2}\frac{M_2}{\Delta} &= -\tfrac{1}{2} \\ \sqrt{8/3}\, h_c\chi_2(\beta l)\frac{Q_0}{\Delta} + \left[2\sqrt{8/3}\, h_c\beta\chi_3(\beta l) + 8R\frac{h_c^3}{h_p^3}\right]\frac{M_0}{\Delta} & \\ - 8R\frac{h_c^3}{h_p^3}\frac{M_2}{\Delta} &= 0 \\ \frac{2}{\sqrt{8/3}}h_c\frac{Q_2}{\Delta} - 6R\frac{h_c^3}{h_p^3}\frac{M_0}{\Delta} + \left[\frac{4}{a\beta} + 6R\frac{h_c^3}{h_p^3}\right]\frac{M_2}{\Delta} &= 0.\end{aligned} \tag{19}$$

IV. SOLUTION OF PROBLEMS

Once the edge loadings are known, the unit stresses in the ceramic cylinders may be calculated. Shell theory assumes that the normal stresses, σ_x and σ_φ, vary linearly through the thickness of the shell from a maximum value at one surface to a minimum value at the other surface. The shearing stress, $\tau = \tau_{xz}$, is assumed to vary across the thickness of the shell according to a parabolic law with a maximum at the center. The variation of these limiting values as a function of distance from the joint is given by (see Ref. 5, pp. 45 and 88)

$$(\sigma_x)_{z=\pm\frac{1}{2}h_c} = \pm\frac{6}{h_c^2} M_x$$

$$(\sigma_\varphi)_{z=\pm\frac{1}{2}h_c} = \left(\nu_c\sigma_x - \frac{E_c}{a} w_c\right)_{z=\pm\frac{1}{2}h_c} \tag{20}$$

$$\tau_{\max} = \frac{3}{2}\frac{Q_x}{h_c},$$

where Q_x, M_x and w_{cx} are the force, moment, and deflection in the cylinder at a distance x from the joint.

4.1 *Radial Unbalance*

Of interest here is the magnitude and distribution of the stresses produced in the cylinders as the radius of cylinder № 2 is increased (Fig. 3a). The cylinders are infinitely long; the expressions for the required quantities are (see Ref. 5, p. 393)

$$\begin{aligned} M_{xi} &= \frac{1}{\beta_i}\left[\beta_i M_0\varphi(\beta_i x) + Q_0\zeta(\beta_i x)\right] \\ w_{ci} &= -\frac{1}{2\beta_i^3 D_c}\left[\beta_i M_0\psi(\beta_i x) + Q_0\theta(\beta_i x)\right] \\ Q_{xi} &= -2\beta_i M_0\zeta(\beta_i x) + Q_0\psi(\beta_i x), \end{aligned} \tag{21}$$

for $i = 1, 2$. Here x is the axial displacement from the cylinder-plate joint.

4.2 *Axial Unbalance*

The effect that varying the length of the middle cylinder has on the stresses in both cylinders № 1 and № 2 is of interest (see Fig. 3b). Cylinder № 1 is infinitely long and, corresponding to (21), the required expressions are

$$\begin{aligned} M_{x1} &= \frac{1}{\beta}\left[\beta M_2\varphi(\beta x) + Q_2\zeta(\beta x)\right] \\ w_{c1} &= -\frac{1}{2\beta^3 D_c}\left[\beta M_2\psi(\beta x) + Q_2\theta(\beta x)\right] \\ Q_{x1} &= -2\beta M_2\zeta(\beta x) + Q_2\psi(\beta x). \end{aligned} \tag{22}$$

Cylinder № 2 is finite in length and the expressions for the required quantities are

$$M_{x2} = \frac{2}{\beta}\left[\Lambda \cos \beta\xi \cosh \beta\xi - \Omega \sin \beta\xi \sinh \beta\xi\right]$$

$$w_{c2} = -\frac{1}{D\beta^3}\left[\Lambda \sin \beta\xi \sinh \beta\xi + \Omega \cos \beta\xi \cosh \beta\xi\right]$$

$$Q_{x2} = -2(\Lambda + \Omega) \sin \beta\xi \cosh \beta\xi + 2(\Lambda - \Omega) \cos \beta\xi \sinh \beta\xi$$

where $\xi = x + l/2$ is the axial displacement measured from the center of the short cylinder and

$$\Lambda = \frac{Q_0 \sin \frac{\beta l}{2} \sinh \frac{\beta l}{2} + \beta M_0 \left(\sin \frac{\beta l}{2} \cosh \frac{\beta l}{2} + \cos \frac{\beta l}{2} \sinh \frac{\beta l}{2}\right)}{\sinh \beta l + \sin \beta l}$$

$$\Omega = \frac{Q_0 \cos \frac{\beta l}{2} \cosh \frac{\beta l}{2} + \beta M_0 \left(\cos \frac{\beta l}{2} \sinh \frac{\beta l}{2} - \sin \frac{\beta l}{2} \cosh \frac{\beta l}{2}\right)}{\sinh \beta l + \sin \beta l}$$

These results are obtained by superposing the solution for the case of bending by uniformly distributed shearing forces Q_0 and the solution for the case of bending by moments M_0 distributed at the ends (see Ref. 5, p. 403).

V. STRESS DISTRIBUTIONS AND MAGNITUDES

Calculations were carried out on an electronic computer to demonstrate the effects of the two types of unbalance. It was decided to use the value $R = 2.1$ for the ratio of elastic moduli corresponding to the Diamonite ceramic cylinders and the Kovar plates employed in the particular tube structure illustrated in Fig. 1. Here Δ is a positive quantity since $\alpha_p > \alpha_c$ and $T_0 > T$. The dimensions of the tube were also chosen to correspond to this practical geometry and the plate thickness was varied.

$$h_c = 0.04 \text{ in.}, \qquad a = 0.22 \text{ in.}, \qquad h_p = 0.01, 0.02, 0.04 \text{ in.}$$

Of interest are the stress distributions in the cylinders, especially the values attained at the seal junctions. These have been obtained for both radial and axial unbalanced seals for the three plate thicknesses.

5.1 *Radial Unbalance*

The stresses in the two cylinders at the cylinder-plate junctions are depicted in Fig. 6. The first graph shows the longitudinal stress at the outer wall of each cylinder; an equal tensile stress occurs at the inner

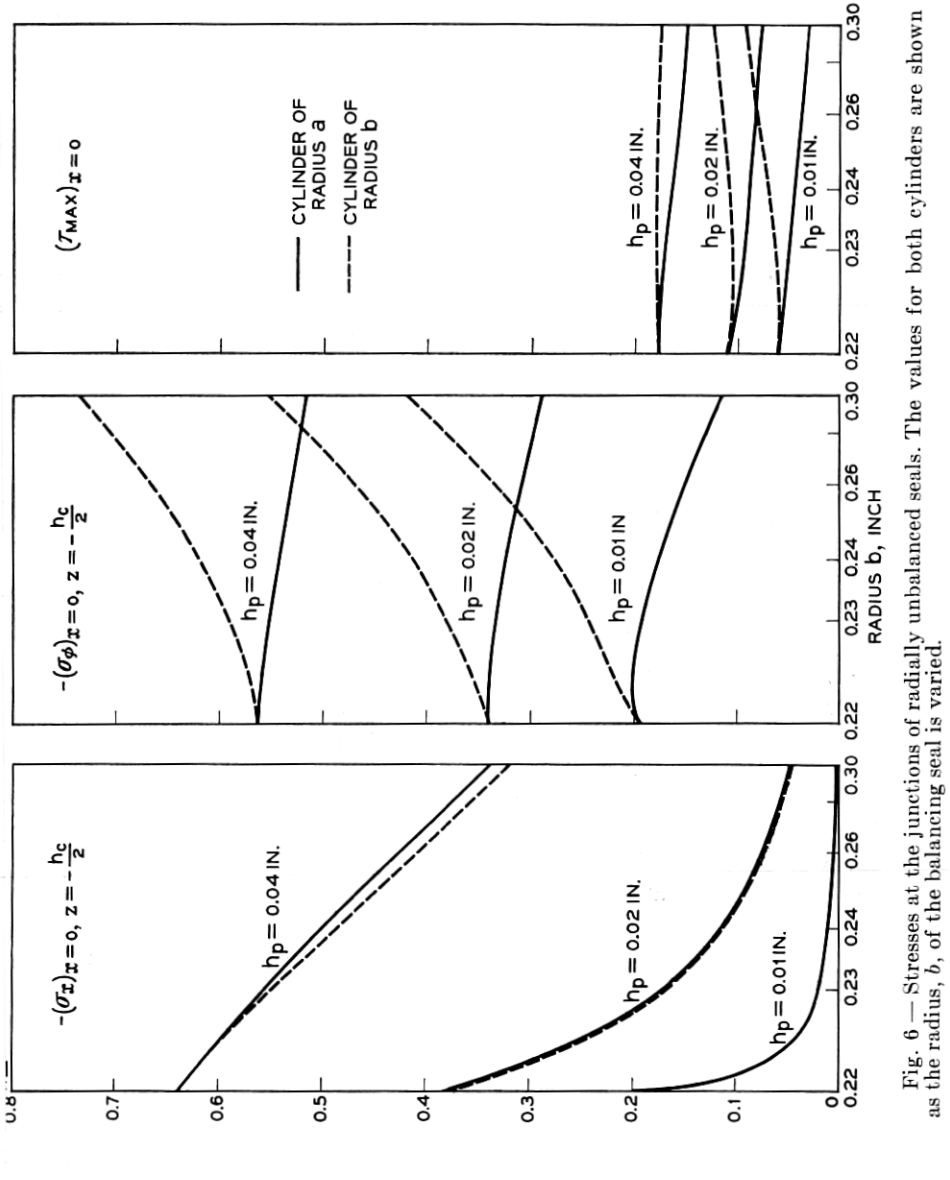

Fig. 6 — Stresses at the junctions of radially unbalanced seals. The values for both cylinders are shown as the radius, b, of the balancing seal is varied.

wall. The circumferential stresses are compressive all across the wall thickness; the maximum numerical values are attained at the outer wall and these are shown in the second graph of Fig. 6. The maximum shear stress acting on the plane of the cylinder-plate junctions is shown in the third graph.

It is seen that as the amount of the unbalance is increased, i.e., b is increased, the junction stresses in the smaller cylinder all decrease. In the larger cylinder the longitudinal stress at the junction decreases, but the circumferential and shear stresses increase. This trend actually continues until the radius of the larger cylinder is several times that of the smaller.

The variation of the stresses as a function of distance from the junction is shown in Fig. 7. It is of special interest to compare the results for completely balanced seal, Fig. 7(a), with those of a completely unbalanced seal, Fig. 7(c).

5.2 *Axial Unbalance*

Figure 8 shows that as the amount of axial unbalance is decreased, i.e., l is increased, the junction stresses in the long cylinder decrease and then increase again to a limiting value. The stresses in the short cylinder are practically the same as those in the long cylinder with the exception of the shearing stresses. The shearing stress in the short cylinder increases with decreasing unbalance to a limiting value. From the standpoint of both cylinders the optimum length for the intermediate or short cylinder appears to be about 0.125 in. The somewhat larger stresses corresponding to the perfectly balanced configuration are attained for l greater than approximately 0.3 in.

If l is allowed to tend to zero the configuration reduces to a perfectly balanced seal with a plate of twice the original thickness. The stresses for a given plate thickness at $l = 0$ must therefore equal the stresses produced in a structure using plates of twice the thickness at very large values of l, say $l = 0.4$. Figure 8 shows this very well.

Figure 9 illustrates the variations in the stress distributions for several lengths of the intermediate cylinder.

VI. DISCUSSION

Practical experience has shown the balanced seal to be stronger than the completely unbalanced seal (*i*) under routine handling conditions, and (*ii*) under thermal shock in subsequent welding operations. In the former case the unbalanced seal is more susceptible to a failure of the bond between the cylinder and plate; in the latter case the weakness is

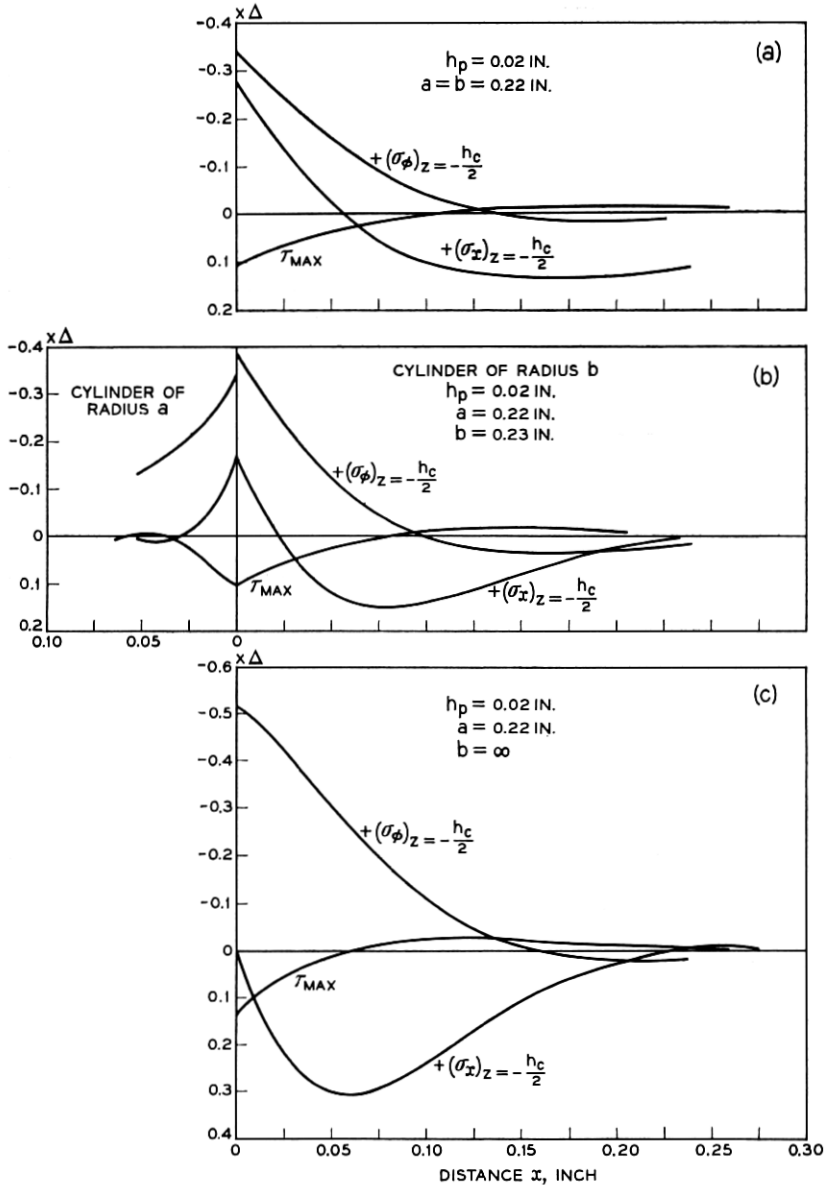

Fig. 7 — Stress distributions showing the effects of various conditions of radial unbalance; (a) completely balanced, (b) slightly unbalanced, (c) completely unbalanced seals.

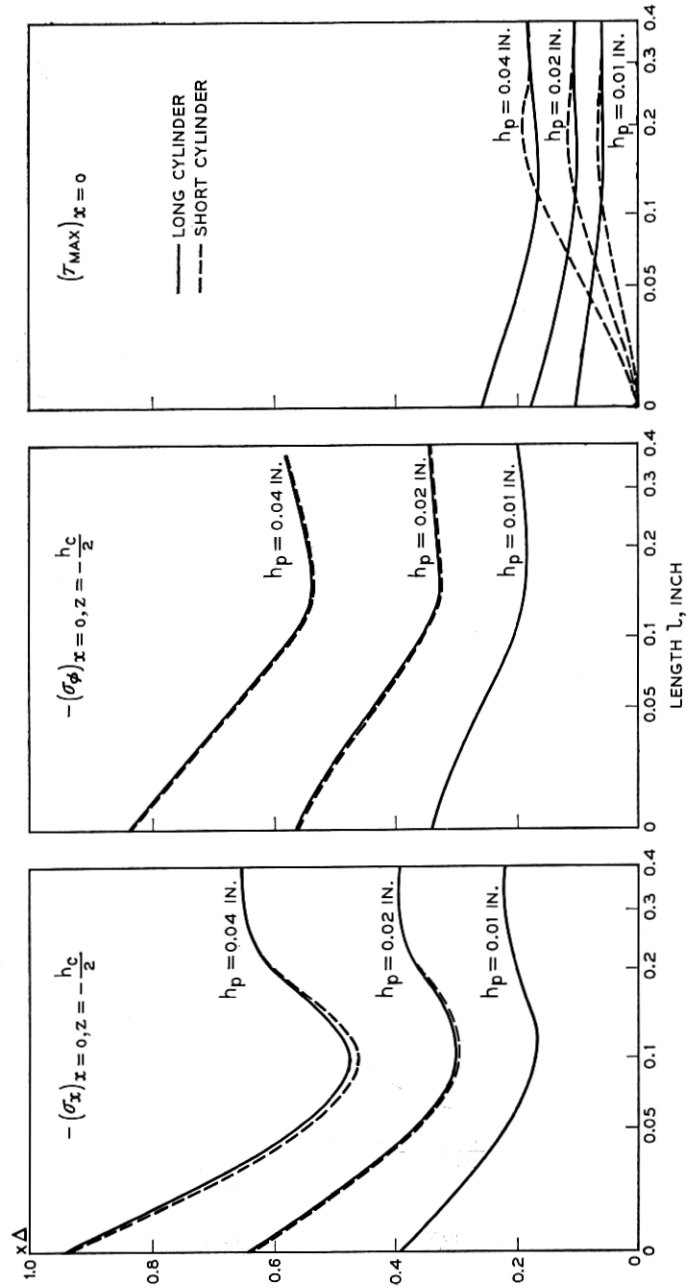

Fig. 8 — Stresses at the junctions of axially unbalanced seals. The values for both cylinders are shown as the length, l, of the intermedate cylinder is varied.

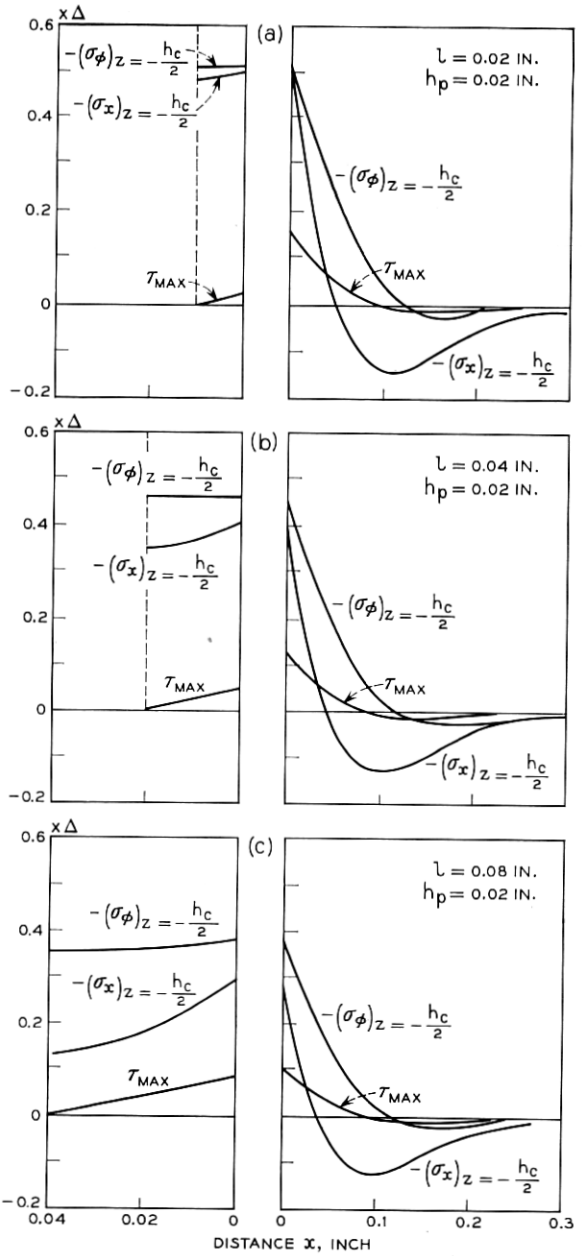

Fig. 9 — Stress distributions showing the effect of varying the length, l, of the intermediate cylinder in an axially unbalanced seal. Note the difference in scale for long (right side) and short (left side) cylinders.

manifested by longitudinal cracks in the unbalanced ceramic cylinder. It is of interest to interpret these facts in the light of the calculated stresses presented above.

Since type (*i*) failures clearly cannot result from compressive circumferential stresses and the longitudinal junction stress is essentially zero for the unbalanced seal, Fig. 7(c), the culprit must be the shear stress at the junction, i.e., the metallized interface fails in shear. Comparison of τ_{max} for the two structures, Fig. 7(a) with Fig. 7(c), shows that indeed its value is about 30 per cent greater for the unbalanced seal than for the perfectly balanced seal.

Type (*ii*) failures occur when the metal plate is raised to a higher temperature than the ceramic cylinder by uneven heating. This introduces tensile circumferential stress in the cylinder which results in longitudinal cracks if the temperature difference is great enough for the residual compressive stress to be sufficiently exceeded. A first approximation to the relative values of these transient stresses is obtained by merely reversing the sign of Δ in the calculations presented. Comparison of Fig. 7(a) and Fig. 7(c) then shows that a much larger circumferential tensile stress would be expected in the unbalanced seal under such a thermal gradient.

If these explanations are valid it may be concluded from Fig. 6 that the balancing cylinder (radius b) is even more effective for $b > a$. For, the magnitudes of the shear and circumferential stresses in the smaller (and more crucial) cylinder decrease as b is increased. The unbalance cannot be made too great, however, as the corresponding stresses in the larger cylinder increase.

In the case of axial unbalance it is clear (Fig. 8) that the intermediate cylinder must have length $l > 0.125$ if the presence of seal at the opposite end is to be negligible. If this inequality is satisfied the susceptibility to failure of either type (*i*) or type (*ii*) is greatly reduced.

VII. ACKNOWLEDGMENT

The authors are happy to acknowledge valuable discussion with W. A. Schlegel. Thanks are also due to Messrs. R. E. Caffrey and W. C. Lo for suggesting the study.

REFERENCES

1. Rawson, G., A Theory of Stresses in Glass Butt Seals, Brit. J. Appl. Phys., **2**, 1951, pp. 151–156.
2. Svenson, N. L., [Comments on Ref. 1], Brit. J. Appl. Phys., **3**, 1952, pp. 30–31.
3. Zaid, M., [Comments on Ref. 1], Brit. J. Appl. Phys., **3**, 1952, pp. 31–32.
4. Lewin, G., and Mark, R., Theory of Dissimilar Tubular Seals of Glass, Ceramics and Metals for Critical Applications, Trans. Fifth National Symposium on Vacuum Technique, 1958 pp. 44–49.
5. Timoshenko, S., *Theory of Plates and Shells*, McGraw-Hill, New York, 1940.
6. Timoshenko, S., and Goodier, J. H., *Theory of Elasticity*, McGraw-Hill, 1951.